

Surface Crystallization of Amorphous Solid Water

Ellen H. G. Backus,¹ Mihail L. Grecea,¹ Aart W. Kleyn,^{1,2} and Mischa Bonn^{1,3}

¹*Leiden Institute of Chemistry, Leiden University, P.O. Box 9502, 2300 RA Leiden, The Netherlands*

²*FOM Institute for Plasma Physics Rijnhuizen, Euratom-FOM Association, P.O. Box 1207, 3430 BE Nieuwegein, The Netherlands*

³*FOM Institute for Atomic and Molecular Physics, Kruislaan 407, 1098 SJ Amsterdam, The Netherlands*

(Received 1 September 2003; published 8 June 2004)

We demonstrate that the crystallization of thin, supported amorphous solid water layers is initiated at the water surface. This is concluded from the observation of sequential crystallization of amorphous water at the surface, in the bulk, and at the water-support interface. A surface nucleation model quantitatively reproduces the observed transformation kinetics at the three sites.

DOI: 10.1103/PhysRevLett.92.236101

PACS numbers: 68.35.Rh, 64.60.Qb, 64.70.Kb, 82.60.Nh

Although solid water in the interstellar medium is predominantly amorphous, crystalline ice has been detected around protostars and in disks around young stars [1]. In this particular environment, the solid water surface covering dust particles [2] provides the catalytic environment for the formation of prebiotic organic molecules in the interstellar medium [3]. The interaction of molecules such as N₂ [4], CHF₂Cl [5], CHCl₃ [this work], and CO [6] with the solid water surface depends critically on the surface structure (crystalline or amorphous). The surface-CO interaction is of special interest, as the first step in the formation of complex organic species is the surface-catalyzed hydrogenation of CO to methanol [7]. It is therefore important to know whether the surface of grains is preferentially amorphous or crystalline. A key question that thus emerges is whether the crystallization is initiated in the bulk or at the surface: if surface crystallization is favored, the particle surface will crystallize first, affecting the surface chemistry. Indeed, it has been proposed that the hydrogen bond rearrangement required for crystallization may occur more readily for the less coordinated water molecules at the surface [8]. On the other hand, Buch *et al.* have calculated that the crystalline geometry is favorable for bulk ice rather than for the surface, implying that commencement of crystallization in the bulk is more likely [9,10].

The energy barrier that must be overcome to form a crystalline nucleus in the amorphous phase is determined by, among other things, a competition between the surface tension that arises between the two phases upon nucleation (counteracting nucleation) and the difference in chemical potential between the two phases (favoring nucleation, as the crystalline phase is thermodynamically most stable). At the surface or interface, the energetic barrier for nucleation may be lower, since only half a sphere has to be formed in order for the nucleation grain to grow [11]. However, it is also clear that the energetics depend subtly on the different contributions from surface—and line—tension that are relevant for the nucleation event [12], as well as the effect of the density difference between the phases [4,5]. Indeed, for thin,

constrained silicon layers, crystallization is nucleated in the bulk of the layer [13]. For amorphous water it is also not clear *a priori* where the crystallization of the layer may start. To investigate the location of the nucleation, we use thin layers of amorphous ice, since for relatively thick layers (>100 molecular layers), the probability of bulk crystallization is large, simply because a large volume is available [4,5,8,14–18], whereas possible surface effects are thickness independent. To suppress the role of the underlying support in the crystallization process, we use a nonepitaxial support, a platinum [Pt(533)] surface to grow the water films on [the 7 Å wide (111) terraces on the stepped Pt(533) surface are twice smaller than the estimated nucleus diameter [17]]. Previous studies [4,8,18] have reported interface crystallization for epitaxial supports. We unambiguously demonstrate that the crystallization commences at the surface in thin films, by simultaneously monitoring the water crystallization kinetics in the bulk, at the surface (vacuum-water interface), and at the interface (water-support interface) of thin amorphous water films.

Nonporous [19] thin films of amorphous solid water of 45 monolayers (ML) [20] (an order of magnitude larger than estimates of the critical nucleus size [17]) were deposited on the support at 100 K using an effusive molecular beam under normal incidence (flux: 0.1 ML s⁻¹) in ultrahigh vacuum [22] (2×10^{-11} mbar). After amorphous film growth, the crystallization is investigated isothermally: the layer is quickly heated to and held at 139 K, where it takes ~500 s to crystallize.

The phase state of the bulk material—amorphous or crystalline—is monitored directly through the OH stretch vibration of water in the layer [23,24]. Reflection absorption infrared (RAIR) spectra [55 scan (20 s) averages] are recorded at 4 cm⁻¹ resolution, under grazing incidence. The IR absorbance A is defined as $A = -\ln(R/R_0)$, with R and R_0 the reflected intensity from the water-covered and bare surface, respectively. Typical absorbance spectra of amorphous solid water and crystalline ice are depicted in Figs. 1(a) and 1(b), respectively. For the former, the spectrum is relatively broad and

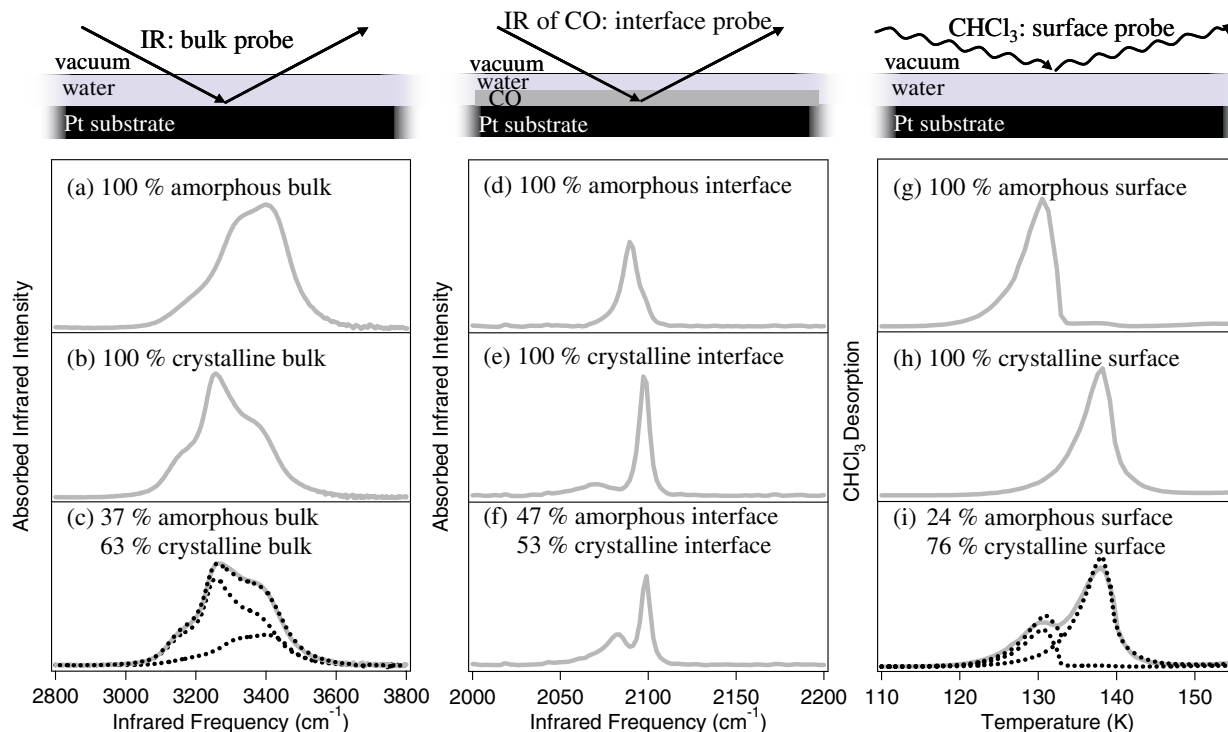


FIG. 1 (color online). Left panel, bulk crystallinity: reflection absorption infrared spectra (139 K) in the OH stretch region of (a) a 45 ML amorphous water layer, (b) a crystalline water layer, and (c) a $(63 \pm 1.5)\%$ crystalline water layer. The dotted black lines in (c) are the fit of a linear combination of the amorphous and the crystalline RAIR spectra and its constituents. The fit reveals that the layer is $(63 \pm 1.5)\%$ crystallized. Middle panel, interface crystallinity: reflection absorption infrared spectra (139 K) in the CO stretch region of CO between the Pt substrate and (d) a 45 ML amorphous water layer, (e) the crystalline water layer, and (f) the water layer for which the RAIR data in the OH stretch region show $(63 \pm 1.5)\%$ bulk crystallinity. Right panel, surface crystallinity: thermal desorption spectra for CHCl_3 from (g) the 45 ML amorphous water layer, (h) the crystalline water layer, and (i) the water layer for which the RAIR data show $(63 \pm 1.5)\%$ bulk crystallinity. The dotted black lines in (i) are the fit with a linear combination of the TPD spectra from the amorphous and the crystalline layer and its constituents. The fit reveals that the surface of the layer is already $(76 \pm 3)\%$ crystallized.

featureless, due to the disordered nature of the layer. Upon crystallization, a narrowing and redshift of the resonance occurs, reflecting the increase in order and stronger hydrogen bonding, respectively. Figure 2 shows that the crystalline-to-amorphous transition is clearly observable in the spectra around 300 s by a spectral shift from ~ 3400 to ~ 3250 cm^{-1} . As shown in Figs. 1(c) and 2(b), the RAIR spectra obtained from a partially crystallized water layer can be described very well by a linear combination of the spectra of the amorphous and the crystalline phase [from Figs. 1(a) and 1(b)] [16,24] at all times, indicating that grain boundary effects are negligible. Also, RAIR spectra of crystalline ice obtained by dosing at 142 K and that obtained by isothermal crystallization of amorphous solid water dosed at 100 K are identical. Thus, the fraction of crystalline ice can be determined within a few percent directly from the relative contributions (corrected for the independently determined difference in infrared absorption cross section). The triangles in Fig. 2(c) depict the bulk crystallinity as a function of time obtained in this way for an amorphous water film initially 45 ML thick.

To probe the phase state of water at the interface, the Pt substrate is covered with carbon monoxide (CO) prior to dosing of water. For epitaxial Pt(111) substrates, for which commencement of crystallization at the interface has been observed [8,18], CO accelerates the crystallization [25,26], because the substrate-water interaction is weakened with CO. In contrast, on the nonepitaxial Pt(533), interfacial CO does not affect the crystallization mechanism, as is evident from a comparison of the measured bulk fraction with and without CO. The frequency of the CO stretch vibration is sensitive to the phase state of the neighboring water: under amorphous solid water it is 2089 cm^{-1} [Fig. 1(d); linewidth, ~ 6 cm^{-1}], while under crystalline ice it is 2098 cm^{-1} [with a small contribution at 2068 cm^{-1} ; Fig. 1(e)]. During the crystallization process, there is continuous intensity transfer from 2089 to 2098 cm^{-1} . As small frequency shifts occur, we use the frequency-integrated changes (between 2050 and 2120 cm^{-1}) in the RAIR spectra as a measure of the interface crystallinity. Figure 1(f) shows the infrared CO stretch absorption for CO under a $(63 \pm 1.5)\%$ crystalline water layer. The CO signal indicates that only

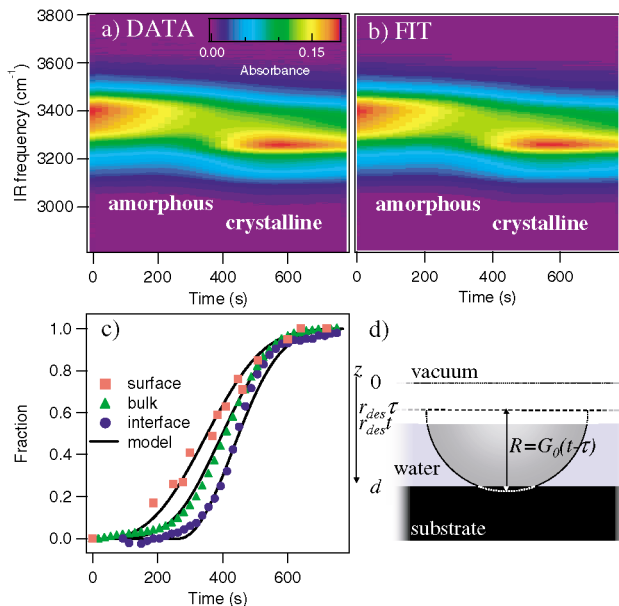


FIG. 2 (color). (a) Measured and (b) fitted (with a linear combination of the amorphous and crystalline RAIR spectra) infrared spectra in the OH stretch region as a function of time for an amorphous water layer with an initial thickness of 45 ML. Since the experiment is performed in vacuum, crystallization is accompanied by simultaneous desorption (sublimation) from the thin film, resulting in a decrease in the RAIR intensity. (c) Experimental (symbols) and calculated (lines) surface, bulk, and interface crystallinity as a function of time for an amorphous water layer with an initial thickness of 45 ML. (d) Schematic representation of the employed model depicting a transformed crystalline region at time t , following the appearance of a crystalline nucleus at the surface at time τ . Crystallization occurs in a thin film of thickness d , which decreases in thickness as desorption is occurring with a rate r_{des} . The nucleus grows with a rate G_0 . The results of this calculation are shown as lines in panel (c).

(53 ± 2)% of the interfacial water has been crystallized. Figure 2(c) shows that the interface crystallinity is always lagging the bulk, indicating that the crystallization does not start at the platinum-water interface. The observed behavior can be explained by either surface crystallization or bulk crystallization. To distinguish between these two possibilities, we also probe the surface crystallinity.

The surface crystallinity of the sample is determined through adsorption and desorption of the surface-structure sensitive probe molecule chloroform, CHCl_3 . This well-established procedure, previously performed with CHF_2Cl [5] and N_2 [4], consists of dosing a monolayer of CHCl_3 at 80 K on a (partially) crystallized ice layer, obtained by interrupting the crystallization through very rapid ($>1 \text{ K s}^{-1}$) cooling. A temperature programmed desorption (TPD) spectrum is obtained by heating the sample at a ramp rate of 0.5 K s^{-1} and detecting the desorbing CHCl_3 with a mass spectrometer. Because of the high heating ramp of 0.5 K s^{-1} , the crys-

tallization and desorption of water do not occur until above 145 K. The right panel in Fig. 1 shows that CHCl_3 desorbs from a fully amorphous layer at 130 K [Fig. 1(g)] and at 140 K from a fully crystalline layer [Fig. 1(h)]. The TPD spectrum from a partially crystallized water layer [Fig. 1(i)] can be described by a linear combination, the relative contributions directly rendering the surface crystallinity. Whereas the RAIR data [Fig. 1(c)] indicate that (63 ± 1.5)% of the bulk has crystallized, the TPD data show that already (76 ± 3)% of the surface has been converted: the surface crystallizes prior to the bulk. Figure 2(c) demonstrates that the surface crystallinity always precedes the bulk. The scatter in the data points is due to the fact that for every point a new water layer has to be used, as during the CHCl_3 TPD the water layer desorbs.

From the sequential crystallization of water at the surface, in the bulk, and at the interface [Fig. 2(c)], it is apparent that there is a significant contribution of surface crystallization to the conversion of the 45 ML thin water layer. This conclusion is further corroborated by the observation that the time-dependent change in desorption rate, reflecting the surface fraction of crystalline ice [8,14,18], is faster than the change in bulk crystallinity. The change in desorption rate is obtained by differentiating the time-dependent intensity of the RAIR spectra data in the OH stretch region. As the desorption rate from amorphous solid water is approximately twice that of crystalline ice [27], the change in the decrease in the RAIR spectra intensity upon crystallization directly reflects the surface composition.

To quantify the crystallization process, we calculate the surface, bulk, and interface fraction of crystalline ice as a function of time [28] for surface nucleation, as schematically depicted in Fig. 2(d), with z the spatial coordinate in the layer. We consider a layer of thickness d (expressed in ML). Crystalline nuclei are formed at the surface at time τ with a probability per unit area per unit time J_0 ($\text{ML}^{-2} \text{ s}^{-1}$). These nuclei subsequently grow at rate G_0 (ML s^{-1}), so that, at a given time $t > \tau$, the radius r of a sphere nucleated at time τ equals $r = G_0(t - \tau)$. As desorption of water occurs simultaneously at rate r_{des} (ML s^{-1}), the thickness at time t equals $(d - r_{des}t)$. The surface and interface fraction are readily calculated from the resulting exposed area of these spheres at either the water-vacuum surface (at $z = r_{des}t$) or water-platinum (at $z = d$) interface [28,29]. The volume fraction is obtained by numerically averaging the slab crystalline fraction (i.e., as a function of depth z) over the instantaneous thickness of the film. The effect of different growth rates for different crystal facets is neglected, as this will average out for the macroscopic quantities of interest.

As shown in Fig. 2(c), the model reproduces the time-dependent surface, bulk, and interface crystallinity with a desorption rate $r_{des} = 0.04 \text{ ML s}^{-1}$, directly obtained from our experiments, a growth rate $G_0 = 0.17 \text{ ML s}^{-1}$,

which is in agreement with Safarik *et al.* [5], and a surface nucleation rate $J_0 = 5.5 \times 10^{-7} \text{ ML}^{-2} \text{ s}^{-1}$. These theoretical results demonstrate that surface nucleation alone can account for the experimental data.

The observation of surface nucleation reflects the energetics of the crystallization process. These energetics include chemical potential, surface tension between the two phases, and density effects. The effect of the density difference between the amorphous and the crystalline phase raises the nucleation barrier. However, this contribution scales with the nucleus volume and therefore has a larger effect for bulk than for surface nucleation. For surface nucleation, additional contributions arise from the three-phase line tension (suppressing surface nucleation) and the surface tension difference between the amorphous-vacuum interface and the crystalline-vacuum interface. Apparently, the sum of the contributions from the line tension and the density difference are smaller than the absolute value of the surface tension between the amorphous and the crystalline phase [12], favoring surface nucleation.

In summary, we demonstrate directly that crystallization of amorphous solid water films starts at the surface of very thin water layers. In addition to the potential implication for the chemistry occurring on interstellar ice particles, our findings may also have consequences for atmospheric processes occurring on ice surfaces.

The authors are grateful to B. Riedmüller, W. Roeterdink, and R. van Schie for experimental help and E. Blokhuis, R. Blosssey, D. Chakarov, E. van Dishoeck, H. Fraser, D. Frenkel, J. Frenken, and B. Kay for helpful discussions. This work is part of the research program of the Foundation for Fundamental Research on Matter (FOM), which is financially supported by the Netherlands Organisation for Scientific Research (NWO).

-
- [1] E. F. v. Dishoeck (to be published).
 - [2] P. Ehrenfreund *et al.*, *Planet. Space Sci.* **51**, 473 (2003).
 - [3] P. Ehrenfreund *et al.*, *Rep. Prog. Phys.* **65**, 1427 (2002).
 - [4] Z. Dohnálek *et al.*, *J. Chem. Phys.* **112**, 5932 (2000).

- [5] D. J. Safarik, R. J. Meyer, and C. B. Mullins, *J. Chem. Phys.* **118**, 4660 (2003).
- [6] A. Al-Halabi, E. F. v. Dishoeck, and G. J. Kroes, *J. Chem. Phys.* **120**, 3358 (2004).
- [7] E. F. v. Dishoeck and M. R. Hogerheijde, in *The Origins of Stars and Planetary Systems*, edited by C. J. Lada and N. J. Kylafis (Kluwer, Dordrecht, 1999), p. 97.
- [8] P. Löfgren *et al.*, *Surf. Sci.* **367**, L19 (1996).
- [9] V. Buch *et al.*, *J. Phys. Chem.* **100**, 3732 (1996).
- [10] B. Rowland *et al.*, *J. Chem. Phys.* **102**, 8328 (1995).
- [11] S. Dietrich, in *Phase Transitions and Critical Phenomena*, edited by C. Domb and J. L. Lebowitz (Academic, London, 1988), Vol. 12, p. 2.
- [12] D. W. Oxtoby, in *Fundamentals of Inhomogeneous Fluids*, edited by D. Henderson (Marcel Dekker, New York, 1992), p. 407.
- [13] L. Zhang *et al.*, *J. Phys. Condens. Matter* **14**, 10083 (2002).
- [14] R. S. Smith *et al.*, *Surf. Sci.* **367**, L13 (1996).
- [15] W. Hage *et al.*, *J. Chem. Phys.* **103**, 545 (1995).
- [16] W. Hage *et al.*, *J. Chem. Phys.* **100**, 2743 (1994).
- [17] P. Ahlström *et al.*, *Phys. Chem. Chem. Phys.* **6**, 1890 (2004).
- [18] P. Löfgren *et al.*, *Langmuir* **19**, 265 (2003).
- [19] K. P. Stevenson *et al.*, *Science* **283**, 1505 (1999).
- [20] The thickness of the water layer is expressed throughout the Letter in monolayers (ML). 1 ML is defined in the standard way as the amount of water adsorbed on the Pt(533) surface that in a thermal desorption experiment gives rise to one desorption feature at 175 K [21] that saturates with exposure, after which multilayer desorption occurs at 160 K.
- [21] H. Ogasawara *et al.*, *Phys. Rev. Lett.* **89**, 276102 (2002).
- [22] B. Riedmüller *et al.*, *Meas. Sci. Technol.* **13**, 141 (2002).
- [23] J. E. Schaff and J. T. Roberts, *J. Phys. Chem.* **100**, 14151 (1996).
- [24] R. S. Smith *et al.*, in *Water in Confining Geometries*, edited by V. Buch and J. P. Devlin (Springer, New York, 2003), p. 336.
- [25] J. Kubota *et al.*, *Chem. Phys. Lett.* **362**, 476 (2002).
- [26] J. Kubota (private communication).
- [27] R. J. Speedy *et al.*, *J. Chem. Phys.* **105**, 240 (1996).
- [28] E. H. G. Backus and M. Bonn, *J. Chem. Phys.* (to be published).
- [29] M. Avrami, *J. Chem. Phys.* **8**, 212 (1940).